Published in final edited form as:

Nat Commun. ; 6: 6846. doi:10.1038/ncomms7846.

Dietary sugar promotes systemic TOR activation in Drosophila through AKH-dependent selective secretion of Dilp3

Jung Kim and **Thomas P. Neufeld***

Department of Genetics, Cell Biology and Development, University of Minnesota, 6-160 Jackson Hall, 321 Church St. SE, Minneapolis, MN 55455 USA

Abstract

Secreted ligands of the insulin family promote cell growth and maintain sugar homeostasis. Insulin release is tightly regulated in response to dietary conditions, but how insulin producing cells (IPCs) coordinate their responses to distinct nutrient signals is unclear. Here, we show that regulation of insulin secretion in Drosophila larvae has been segregated into distinct branches: whereas amino acids promote secretion of Drosophila insulin-like peptide 2 (Dilp2), circulating sugars promote selective release of Dilp3. Dilp3 is uniquely required for sugar-mediated activation of TOR signaling and suppression of autophagy in the larval fat body. Sugar levels are not sensed directly by the IPCs, but rather by the adipokinetic hormone (AKH)-producing cells of the corpora cardiaca, and we demonstrate that AKH signaling is required in the IPCs for sugar-dependent Dilp3 release. Thus, IPCs integrate multiple cues to regulate secretion of distinct insulin subtypes under varying nutrient conditions.

Keywords

insulin; Drosophila insulin-like peptide (Dilp); adipokinetic hormone (AKH); autophagy; target of rapamycin (mTOR/TOR); secretion

INTRODUCTION

Insulin signaling is a conserved mechanism regulating cell growth, differentiation and development. Under feeding conditions, insulin is secreted into the circulatory system and activates insulin receptors in peripheral cells[1]. Subsequent activation of downstream components of the insulin pathway such as phosphoinositide 3-kinase (PI3K), AKT, and target of rapamycin (TOR) leads to uptake of nutrients and stimulation of protein and lipid synthesis. Insulin signaling also suppresses autophagy, a catabolic mechanism that produces an alternative source of nutrients through degradation of cytoplasmic components[2]. This

*Corresponding author. neufe003@umn.edu, Tel: 612-625-5158, Fax: 612-626-5652.

AUTHOR CONTRIBUTIONS

JK performed the experiments. JK & TPN designed and interpreted experiments and wrote the manuscript.

COMPETING FINANCIAL INTERESTS

The authors declare that they have no competing financial interests.

process involves sequestration of cytoplasm within vesicular structures called autophagosomes, which fuse with lysosomes containing digestive enzymes. Induction of autophagy is inhibited by TOR, which in turn is activated both by insulin signaling and directly by intracellular nutrients, particularly amino acids.

In addition to these effects on cell growth and autophagy, insulin also plays a well characterized role in controlling sugar levels in the blood. In mammals, pancreatic beta cells release insulin in response to high levels of glucose, leading to uptake of glucose by other cells in the body to decrease sugar levels. When the level of glucose is low, pancreatic alpha cells secrete glucagon, a G protein-coupled receptor (GPCR) ligand that triggers glycogenolysis and gluconeogenesis to increase sugar levels.

Basic mechanisms of insulin and glucagon signaling are conserved in Drosophila, which provides a useful animal model system to investigate the effects of these hormones on growth and metabolism[3–5]. Drosophila insulin-like peptides (Dilps) regulate cell growth and aging, and they maintain normal sugar levels in the hemolymph, the circulating fluid in insects. Eight Dilps have been identified, of which Dilp2, Dilp3 and Dilp5 are produced in the insulin producing cells (IPCs) of the brain. Ablation of the IPCs causes hyperglycemia in Drosophila larvae, and this phenotype can be rescued by ectopic expression of Dilp2[6]. In addition, the corpora cardiaca (CC) in the ring gland generates the GPCR ligand adipokinetic hormone (AKH), which has homologous functions to glucagon, contributing to sugar homeostasis as well as regulation of fat stores[7,8].

The secretion of Dilps from the IPCs is regulated by dietary nutrients through non-autonomous relay mechanisms. In response to dietary amino acids, the fat body produces an undefined signal that promotes Dilp2 secretion into the hemolymph[9]. In adult flies, the fat body secretes the JAK/STAT ligand Unpaired 2 in response to dietary nutrients, which also stimulates Dilp2 release[10]. Whether secretion of other Dilps is controlled through similar mechanisms is unclear, and the direct effects of hemolymph sugar levels on Dilp release remain poorly understood.

Here, we show that Dilp2 and Dilp3 differ in their regulation by distinct classes of nutrients: whereas Dilp2 secretion responds selectively to amino acids, secretion of Dilp3 is stimulated primarily by glucose and trehalose, the major sugar present in Drosophila larval hemolymph. Further, we demonstrate that trehalose stimulates the corpora cardiaca to release AKH, which then acts directly on the IPCs to promote secretion of Dilp3. Trehalose-mediated Dilp3 secretion from the IPCs leads to upregulation of TOR signaling and suppression of autophagy in the larval fat body, and is required for sugar homeostasis and normal rates of larval development under nutritional stress. We propose that coupling AKH release to the selective secretion of Dilp3 plays a critical role in promoting sugar homeostasis under the conditions of high insulin signaling required for rapid cell growth during larval development.

RESULTS

Trehalose promotes activation of TOR in the larval fat body

To examine how systemic insulin signaling activity is influenced by sugar levels in Drosophila larvae, we developed an e*x vivo* culture system in which dissected larval carcasses are incubated in medium with varying sugar concentrations. As a measure of insulin signaling in peripheral tissues, we first examined the activity of TOR in the larval fat body, a site of high sensitivity to insulin signaling. Incubation of inverted larval carcasses in M3 medium, a commonly-used insect cell culture medium, led to a rapid decrease in TOR-dependent phosphorylation of S6K Thr398 in fat body extracts (Fig. 1a). We refer hereafter to this phosphorylation signal as fb-TOR activity. In contrast, fb-TOR activity was maintained when M3 medium was supplemented with glucose or trehalose, the two main sugars present in Drosophila hemolymph (Fig. 1A, Supplementary Fig. 1a, b). Sucrose, which is not a constituent of hemolymph, did not support fb-TOR activity (Supplementary Fig. 1b). As trehalose, but not glucose, promoted fb-TOR activity in the range of its normal physiological concentration in larval hemolymph[11], we focused our further analysis on this disaccharide.

The effects of trehalose *ex vivo* were recapitulated in *in vivo* feeding experiments. Larvae raised on agar/tryptone food containing trehalose showed dose-dependent activation of TOR in the fat body compared to food lacking trehalose (Fig. 1a). As a physiological readout of this pathway, we monitored the effect of trehalose on induction of autophagy, which is inhibited by TOR signaling. Both *in vivo* feeding and *ex vivo* incubation in the absence of trehalose led to the formation of mCherry-Atg8-positive autophagosomes and autolysosomes throughout the larval fat body within four hours. Inclusion of trehalose in these experiments prevented autophagy induction (Fig. 1b). *Ex vivo* incubation in a more severe starvation medium (EBSS supplemented with leucine) also led to autophagy induction that was suppressed by trehalose (Supplementary Fig. 1c). Together, these data suggest that both dietary and circulating hemolymph trehalose can promote TOR activation in the larval fat body.

Trehalose regulates systemic insulin signaling

Several lines of evidence indicated that activation of TOR by trehalose may be mediated by insulin signaling. First, trehalose-dependent TOR activation was strongly inhibited by expression in the fat body of a dominant-negative subunit of PI 3-kinase, a central component of the insulin pathway (Fig. 1c). Second, the *ex vivo* requirement for trehalose to maintain fb-TOR activation and suppress autophagy was bypassed by inclusion of human insulin in the medium (Fig. 1b,d). Finally, trehalose promoted phosphorylation of Akt on Ser505, a site of activation regulated by insulin signaling (Supplementary Fig. 1d).

Of the eight Drosophila insulin-like proteins, Dilp2, Dilp3 and Dilp5 are expressed in twin clusters of IPCs within the central nervous system. To examine the potential involvement of these brain-derived Dilps in mediating the systemic effects of trehalose, we first tested whether the CNS itself is required for trehalose-stimulated activation of TOR. Whereas trehalose promoted dose-dependent S6K phosphorylation in the fat body of complete

carcasses, removal of the brain and associated ring gland complex abrogated this response (Fig. 2a). Trehalose also failed to suppress autophagy induction in the fat body of brain-less larval carcasses (Fig. 2b). To ask whether soluble factors from the brain are released into the media, we pretreated M3+trehalose medium by incubation with larval brain/ring gland complexes. This conditioned medium was able to fully activate S6K phosphorylation in the fat body of brain-less carcasses (Fig. 2c). In contrast, medium conditioned with CNS complexes from larvae mutant for *Dilps1–5* and *Dilp7* was significantly less effective in this assay. These results indicate that trehalose-dependent activation of TOR in the larval fat body is a non-autonomous response requiring a CNS-derived signal, and that one or more of the brain-derived Dilps are required for a significant portion of this signal.

Trehalose activates TOR via selective secretion of Dilp3

The requirement for the central nervous system implicates Dilp2, Dilp3 and/or Dilp5 in trehalose-responsive signaling. To directly test the potential role of these factors, we examined the effects of trehalose in mutant animals individually lacking each Dilp. Whereas homozygous *Dilp2* and *Dilp5* mutants each showed normal fat body TOR activation following *ex vivo* incubation in trehalose-containing media, this response was defective in *Dilp3* mutant larvae (Fig. 3a). Similarly, mutation of *Dilp3* but not *Dilp2* or *Dilp5* strongly reduced fb-TOR signaling *in vivo* in response to inclusion of trehalose in the diet (Fig. 3b). Thus, we conclude that trehalose elicits systemic insulin signaling primarily through Dilp3.

Géminard and coworkers showed previously that dietary amino acids promote secretion of Dilp2 from the IPCs, and that Dilp2 protein accumulates to high levels in these cells in response to amino acid starvation[9]. We used a similar immunostaining approach to examine the effects of trehalose on Dilp accumulation and release. Following *ex vivo* incubation in M3 medium supplemented with trehalose, protein levels of both Dilp2 and Dilp3 were low in the IPCs, as assayed by antibodies specific for either Dilp2 or Dilp3 (see Supplementary Figs. 2a,b for antibody control experiments). In contrast, incubation in medium lacking trehalose led to a marked accumulation of Dilp3 but not Dilp2 in these cells (Fig. 4a). Similar effects were observed *in vivo*: staining intensity of both Dilps was low in the IPCs of larvae raised on food rich in amino acids and trehalose, and removal of trehalose from the diet led to accumulation of Dilp3 but not Dilp2 (Fig. 4b). Starvation for amino acids had the opposite effect, increasing the intensity of Dilp2 staining, as reported, but not of Dilp3. The expression of Dilp2 and Dilp3 mRNA was unchanged in response to these dietary conditions (Fig. 4c). Finally, larvae raised on food containing trehalose had a higher level of circulating Dilp3 protein in the hemolymph (Fig. 4d), consistent with the low Dilp3 levels in the IPCs under these conditions. Thus, whereas the mRNA levels of both Dilp2 and 3 have been shown to increase in response to a high sugar diet and to correlate with glucose and trehalose hemolymph concentrations[12], our data indicate that only Dilp3 is regulated by sugar at the level of secretion. Taken together, we conclude that secretion of Dilp2 and Dilp3 is independently regulated by amino acids and trehalose, respectively.

How might different nutrient cues promote selective secretion of distinct insulin-like peptides? Individual secretion granules containing Dilps can be visualized within the IPCs by high-powered confocal imaging. Analysis of brains double-labeled for Dilp2 and Dilp3

revealed that while some of these granules contain both Dilps, many contain largely either Dilp2 or Dilp3 (Fig. 4e, Supplementary Fig. 2c,d). Interestingly, granules containing Dilp2 or Dilp3 tend to segregate to distinct regions of the cell. In addition, many individual IPCs show a clear bias in the levels of one Dilp over another. Thus, activation of distinct release pathways and/or subclasses of IPCs may contribute to these nutrient-selective responses.

An AKH-Dilp3 relay mediates trehalose-dependent TOR signaling

In mammals, ATP-sensitive potassium channels in the pancreatic beta cells play a critical role in sensing glucose levels and regulating insulin secretion. Interestingly, Drosophila homologs of these channel subunits are absent from larval IPCs, but instead are specifically expressed in the corpora cardiaca (CC) cells of the ring gland[7]. These cells express the glucagon-like hormone AKH, and they make contact with processes from the IPCs. We found that RNAi-mediated depletion of AKH in the CC, or ablation of the CC itself, inhibited fat body TOR activation in response to trehalose (Fig. 5a; see Supplementary Fig. 3a for depletion and ablation controls). Null mutation of the AKH receptor *AKHR* showed a similar block in TOR activation (Fig. 5b). Conversely, overexpression of AKH increased TOR activity in both the presence and absence of trehalose (Fig. 5c).

The influence of AKH signaling on trehalose-dependent TOR activation suggested that secretion of AKH may be regulated by trehalose. Although previous studies using fluorescent calcium sensors indicate that acute reduction in trehalose may stimulate secretion from CC cells[7], AKH protein levels in the CC were markedly increased following a 2-hr incubation in medium lacking trehalose (Fig. 6a). This accumulation of AKH can be attributed to decreased secretion rather than increased production, as cycloheximide was included in these experiments to inhibit synthesis of new protein. Furthermore, CC-specific expression of the exocytosis inhibitor tetanus toxin, which has been shown to inhibit AKH secretion[13], prevented the reduction in AKH staining in response to trehalose (Fig. 6a). To confirm that release and diffusion of AKH is required for TOR activation in the fat body, we depleted AKH from the medium by adding a blocking antibody against AKH, which led to a dose-dependent decrease in trehalose-stimulated fb-TOR activity (Fig. 6b). Altogether, these results indicate that secretion of AKH from the CC is an essential intermediary step in trehalose-responsive TOR activation.

The similar effects of AKH and Dilp3 are consistent with these factors acting in a common pathway to communicate trehalose levels to peripheral tissues. We therefore asked whether AKH signaling is required in the IPCs for fb-TOR activity. Indeed, IPC-specific knockdown of AKHR significantly inhibited activation of TOR in the fat body in response to trehalose (Fig. 7a). These results support the possibility that AKH signaling in the IPCs may be necessary for the trehalose-stimulated release of Dilp3. Consistent with this hypothesis, Dilp3 protein accumulated to high levels in the IPCs in response to depletion of AKH in the CC, in AKH receptor null mutants, and in response to depletion of AKHR specifically in the IPCs (Fig. 7b). These manipulations had no effect on Dilp3 mRNA levels (Fig. 7c). We conclude that the IPCs are important targets of AKH signaling, releasing Dilp3 in response to a trehalose-AKH relay from the CC cells.

Dilp3 effects developmental rate and sugar homeostasis

Although insulin signaling is essential for normal growth and development, mutation of most individual Dilps has surprisingly little developmental effect, presumably due to redundancy and compensation between these factors[14,15]. In particular, mutants lacking *Dilp3* develop with normal timing and show only a modest reduction in fecundity. We confirmed this lack of effect on developmental rate when *Dilp3* mutant and control animals were raised on rich medium supplemented with yeast. However, growth on medium lacking yeast resulted in a 30-hr delay in development in *Dilp3* mutant compared to control animals (Fig. 8a). These results reveal a cryptic growth requirement for Dilp3, presumably made evident here due to reduced levels of Dilp2 and/or Dilp5 under conditions of low amino acids. Interestingly, *AKHR* mutants showed a similarly enhanced developmental delay in the absence of dietary yeast (Supplementary Fig. 3b), further supporting that AKH and Dilp3 function in a common pathway. In addition, levels of circulating trehalose were significantly higher in *Dilp3* mutant larvae than controls, particularly under the fed conditions required for Dilp3 release (Fig. 8b, Supplementary Fig. 3c). Altogether, these results are consistent with a central role for Dilp3 in mediating growth and metabolism in response to dietary sugar.

DISCUSSION

The dual roles of insulin in promoting both cell growth and sugar homeostasis impose a unique challenge during periods of high growth such as larval and fetal development: sustained insulin signaling is required for normal developmental growth, yet circulating sugar concentrations must be maintained at a steady level under varying nutritional conditions. The results presented here suggest that in Drosophila larvae, this challenge is met in part through the coupled secretion of Dilp3 and AKH (Fig. 8c). This allows for normal hemolymph sugar concentrations despite relatively high Dilp levels, due to the counteracting effects of AKH. Although these hormones have opposing effects on hemolymph sugar concentrations akin to those of mammalian insulin and glucagon, their mechanisms of action are distinct. Ablation of the IPCs or deletion of Dilps 1–5 leads to increased hemolymph sugar concentrations[6,14], likely reflecting a conserved role of Dilps in promoting glucose utilization and uptake through trafficking of glucose transporters[16]. In contrast, manipulation of AKH signaling, through CC ablation or AKH overexpression, strongly effects the concentration of trehalose, but has little or no effect on glucose levels[8]. This hypertrehalosemic effect of AKH is widely conserved in insects, and reflects the unique features of trehalose as both a circulating and storage form of carbohydrate. Due to the non-reactive, non-reducing properties of trehalose, its concentration can vary over a much wider range than glucose without causing cellular damage[17]. Hemolymph trehalose concentrations are commonly more than 10-fold higher than those of glucose, presumably due to the rapid conversion of glucose to trehalose in the fat body by trehalose-6-phosphate synthase[18]. This may counteract the low efficiency of insect open circulatory systems, bringing high concentrations of trehalose directly to cells, each molecule of which can be cleaved within the cell to provide 2 glucose molecules as needed. Thus, the effect of AKH on trehalose and total sugar levels likely masks smaller changes in glucose concentrations that may be more directly regulated by Dilps. Finally, in contrast to their opposing effects on

sugar homeostasis, it is notable that AKH and insulin signaling act in the same direction to promote expression of the α-glucosidase gene *target of brain insulin (tobi)*[19]. Together with the stimulation of Dilp3 secretion by AKH described here, these findings indicate that in addition to its glucagon-like role, AKH may also function as a homolog to glucagon-like peptide-1 (GLP-1), a positive regulator of mammalian insulin signaling[20].

In contrast to the effect of trehalose as an autophagy suppressor described here, trehalose has been shown to activate autophagy in cultured mammalian cells, through undefined mechanisms[21]. Recently, Inoue and coworkers demonstrated that sugars such as trehalose, sucrose and raffinose that cannot be hydrolyzed by mammalian cells induce autophagy, whereas cleavable disaccharides such as maltose and fructose do not[22]. In this regard, it is notable that both the larval fat body and the CC cells express trehalase, which catalyzes conversion of trehalose to glucose[7]. Indeed, it is unclear whether trehalose might be directly sensed and imported by the CC, or first converted to glucose through trehalases expressed on the cell surface[17].

The division of labor between Dilp2 and Dilp3 in responding to amino acids and sugars likely contributes to the ability of insulin signaling to balance growth and metabolic requirements, allowing overall insulin signaling to remain high in growing larvae, while individual Dilps fluctuate in response to specific changes in nutrient conditions. This view implies that each of the eight Dilps may have evolved unique physiological functions in line with their specific mode of regulation. Whether different Dilps are functionally distinct remains poorly understood, but key differences between Dilp2 and Dilp3 may make them uniquely suited for growth and sugar homeostasis, respectively. For example, Dilp2 has been shown to have the strongest growth-promoting properties of Dilps1–7 when overexpressed during larval development[23]. Notably, the insulin-binding factors Imp-L2 and dALS are able to form protein complexes with Dilp2 but not Dilp3, whereas Dilp3 but not Dilp2 interacts strongly with the insulin receptor decoy SDR[24,25], suggesting that individual Dilps may engage the insulin receptor in qualitatively different ways. Interestingly, expression of Dilp5 is up-regulated in *dilp2* mutants and down-regulated in *dilp3* mutants[15], indicating that these factors can have different and even opposing cellular effects, despite utilizing the same insulin receptor. Finally, recent studies have shown that selective outputs of insulin signaling can show distinct responses to transient vs. sustained patterns of receptor activation[26]. In this regard, we note that although we show here that Dilp3 but not Dilp2 is involved in acute responses to altered sugar levels, a chronic high sugar diet can increase the circulating levels of overexpressed Dilp2[12,27], and mutation of *dilp2* leads to increased hemolymph trehalose levels by adulthood[15]. As secretion of Dilp2 is promoted by activation of TOR in the fat body[9], our finding that Dilp3 mediates fb-TOR activation by trehalose suggests that acute and chronic responses to sugar may be linked by a feed-forward mechanism, whereby initial secretion of Dilp3 promotes subsequent Dilp2 secretion and further amplification of insulin signaling.

The selective secretion of Dilp2 and Dilp3 in response to distinct nutritional cues suggests that Dilp peptides contain unique sequence or structural cues targeting them to distinct secretory pathways, or that homophilic interactions promotes self-sorting of these peptides. Indeed, confocal analysis revealed clear segregation of Dilp2 and Dilp3 into different

granules and intracellular regions. Selective secretion in response to a number of distinct stimuli has been described in eosinophils and mast cells: through a process known as piecemeal degranulation, specific cytokines are sequestered from secretion granules and shuttled to the plasma membrane in distinct secretory vesicles[28]. This sequestration step involves direct ligand-receptor interaction within secretory pathway compartments. Similarly, release of specific classes of neurotransmitters from individual nerve terminals can be differentially stimulated in response to varying levels of Ca^{2+} concentration[29]. In mouse islet beta cells, glucagon-like peptide-1 was recently shown to selectively promote the secretion of newly synthesized secretory granules over that of granules previously docked at the plasma membrane[30]. As the three receptors shown to regulate Dilp secretion – GABA-R[10], adiponectin R[31], and AKHR (present study) – are each members of the GPCR family, it will be interesting to investigate how different modes of downstream signaling ultimately affect selective Dilp release.

METHODS

Drosophila strains

The following *D. melanogaster* strains were used: *AKHR[1], AKHR[revA]* (ref. 32, gift of R. Kühnlein, Max Planck Institute, Göttingen, Germany); *AKH[KK105063]* and *AKHR[KK109300]* RNAi lines (Vienna Drosophila RNAi Center, Vienna, Austria); UAS-mChAtg8a (ref. 33); Akh-GAL4.L, Cg-GAL4.A, Df(2L)Exel7027, Dilp2-Gal4.R, *Dilp2[1], Dilp3[1], Dilp5[1], Df(3L)Dilp1–4 Dilp5[4] Dilp7[1]*, Oregon-R-C, UAS-Akh.L, UAS-Dp110[D954A], UAS-rpr.C, and UAS-TeTxLC.(−)Q were obtained from the Bloomington Drosophila Stock Center (Bloomington, IN).

Larval culture

Embryos were collected for 3–5 hours on standard fly food. For *in vivo* feeding experiments, early L3 larvae (85 – 90 hr after egg laying (AEL) 25 °C) were transferred to agar/tryptone medium containing 5.76 mg/ml of agar, 17 mg/ml of tryptone, 2 mg/ml of leucine with or without 26.6 mg/ml of trehalose for 15–17 hr prior to dissection.

For *ex vivo* carcass incubation experiments, L3 larvae (72–77 hr AEL) were transferred to fresh standard fly food supplemented with granular yeast. After 24 hr, seven larvae per condition were bisected and inverted, and digestive tracks removed. Dissected carcasses were incubated with nutation at room temperature in 1 mL of Shields and Sang M3 Insect Medium (not serum supplemented) with or without trehalose (40 mg/ml or otherwise noted) for 2 hr (for western blotting) or 4 hr (autophagy experiments). M3 medium (S3652), trehalose (T0167), human insulin solution (I9278), Earle's Balanced Salts Solution (E3024) and L- Leucine (L8000) were from Sigma-Aldrich (St. Louis MO).

Conditioned medium was made by incubating brain and ring gland complexes from ten larvae for 2 hr in 1mL of M3 medium containing 40 mg/ml trehalose. The recovered medium was used immediately for incubation with carcasses from which the brain was removed.

Immunoblotting

Fat bodies from 5 larvae per sample were dissected in PBS and lysed directly in SDS sample buffer, with three or more biological replicates used for each experiment. Extracts were boiled 3 minutes, separated by polyacrylamide gel electrophoresis, and transferred to Immobilon-P membranes (Millipore, Billerica MA). Circulating Dilp3 levels were determined from hemolymph of 10 larvae per sample, diluted 1:100 in PBS and spotted (1 uL) onto methanol-soaked Immobilon-P membranes (Millipore, Billerica MA). Air-dried membranes were blocked in PBT + 5% BSA, and incubated overnight in blocking solution containing primary antibody. Signals were visualized using SuperSignal West Pico chemiluminescent substrate (Thermo Scientific, Rockford, IL) with BioMax Light (Kodak, Rochester NY) or HyBlot CL autoradiography film (Denville Scientific, Metuchen NJ), and quantitated using Adobe Photoshop software. Antibodies used were rabbit anti-phospho-T398 dS6K (1:250), rabbit anti-phospho-S505 dAkt (1:1,000), (both from Cell Signaling Technology, Beverly MA), rabbit anti-Dilp3 (1:1,000; gift of J. Veenstra, Université Bordeaux, Talence, France, ref. 34), and mouse anti-beta-tubulin E7 (1:1,000; Developmental Studies Hybridoma Bank, Iowa City IA).

Confocal imaging

Samples were prepared for confocal imaging as follows. 7–10 larvae were bisected and inverted in PBS, fixed 20 min in 4% paraformaldehyde / PBS, washed extensively in PBS + Triton X-100 (PBT; 0.3% or 0.1% for imaging IPCs or CCs, respectively), blocked in PBT + 5% bovine serum albumin (BSA), and incubated overnight in blocking solution containing primary antibody. After four washes in PBT, samples were incubated 2hr in blocking solution containing secondary antibody and washed four times. Carcasses after incubation *ex vivo* were directly used for fixation. For autophagy detection, samples were prepared, fixed, and washed as described above. Fixed tissues were dissected in PBS, mounted in Vectashield (Vector Labs, Burlingame, CA), and confocal images were collected on a Zeiss LSM710 confocal microscope and processed with Adobe Photoshop. The following antibodies were used for imaging experiments: rabbit anti-AKH (1:500), rabbit anti-Dilp2 (1:500), rabbit anti-Dilp3 (1:500), mouse anti-Dilp3 (1:500; all gifts of J. Veenstra, Université Bordeaux, Talence, France, ref. 34), rat anti-Dilp2 (1:500; gift of P. Leopold, Université de Nice, Nice, France, ref. 9), rabbit anti-AKH (1:500; gift of J. Park, University of Tennessee, Knoxville, TN, ref. 8).

Sugar measurement

Hemolymph sugar concentrations were determined as described previously[35]. Briefly, 1 uL of hemolymph was obtained from 9–10 L3 larvae and mixed with 9 uL of trehalase buffer (5 mM Tris pH 6.6, 137mM NaCl, 2.7 mM KCl). After incubation for 5 min at 95 °C and centrifugation for 10 min at 4 °C at 15,000 rpm, the supernatant was used for sugar measurement. Glucose (GO) Assay Kit (GAGO-20, Sigma-Aldrich, St. Louis MO) was used according to manufacturer's instructions to measure glucose. For trehalose measurements, supernatants were first incubated at 37 °C overnight with trehalase (T8778-1UN, Sigma-Aldrich Co. St. Louis, MO), and glucose levels were then measured as above. Samples were

read in 96-well plates (3641, Corning Life Sciences, Corning NY) at 540 nm using a Victor 3V 1420 multilabel counter (Perkin Elmer, Waltham MA).

mRNA measurement

25 brains per sample were dissected in PBS, and total RNA was isolated using a Direct-zol RNA MiniPrep kit (R2050, Zymo Research, Irvine CA). RevertAid First Strand cDNA Synthesis Kit (K1621, Thermo Scientific, Pittsburgh PA) was used for reverse transcription of 600 ng of total RNA. Products were amplified by PCR using Ex Taq DNA Polymerase (RR001, Clontech Laboratories, Mountain View CA) for 34 reaction cycles, which was determined in control experiments to be within a linear range of amplification. Primer sequences were as follows: Dilp2-F 5'-CTGAGTATGGTGTGCGAGGA-3'; Dilp2-R 5'-CAGCCAGGGAATTGAGTACAC-3'; Dilp3-F 5'-GACCAAGAGAACTTTGGACCC-3'; Dilp3-R 5'-CAGCACAATATCTCAGCACCTC-3'; Rp49-F 5'-CGGATCGATATGCTAAGCTGT-3'; Rp49-R 5'-GCGCTTGTTCGATCCGTA-3'.

Supplementary Material

Refer to Web version on PubMed Central for supplementary material.

ACKNOWLEDGEMENTS

We would like to thank Drs. Ronald Kühnlein, Pierre Leopold, Jae Park and Jan Veenstra for generous gifts of flies and antibodies. We also thank the Vienna Drosophila RNAi Center, the Bloomington Drosophila Stock Center and the Developmental Studies Hybridoma bank at the University of Iowa for providing fly stocks and antibodies. This work was supported by NIH grant R01 GM62509 to TPN.

REFERENCES

1. Prentki M, Matschinsky FM, Madiraju SR. Metabolic signaling in fuel-induced insulin secretion. Cell Metab. 2013; 18:162–185. [PubMed: 23791483]
2. Kim KH, Lee MS. Autophagy--a key player in cellular and body metabolism. Nature reviews. Endocrinology. 2014; 10:322–337. [PubMed: 24663220]
3. Owusu-Ansah E, Perrimon N. Modeling metabolic homeostasis and nutrient sensing in Drosophila: implications for aging and metabolic diseases. Disease models & mechanisms. 2014; 7:343–350. [PubMed: 24609035]
4. Kannan K, Fridell YW. Functional implications of Drosophila insulin-like peptides in metabolism, aging, and dietary restriction. Frontiers in physiology. 2013; 4:288. [PubMed: 24137131]
5. Bednarova A, Kodrik D, Krishnan N. Unique roles of glucagon and glucagon-like peptides: Parallels in understanding the functions of adipokinetic hormones in stress responses in insects. Comparative biochemistry and physiology. Part A, Molecular & integrative physiology. 2013; 164:91–100.
6. Rulifson EJ, Kim SK, Nusse R. Ablation of insulin-producing neurons in flies: growth and diabetic phenotypes. Science. 2002; 296:1118–1120. [PubMed: 12004130]
7. Kim SK, Rulifson EJ. Conserved mechanisms of glucose sensing and regulation by Drosophila corpora cardiaca cells. Nature. 2004; 431:316–320. [PubMed: 15372035]
8. Lee G, Park JH. Hemolymph sugar homeostasis and starvation-induced hyperactivity affected by genetic manipulations of the adipokinetic hormone-encoding gene in Drosophila melanogaster. Genetics. 2004; 167:311–323. [PubMed: 15166157]
9. Geminard C, Rulifson EJ, Leopold P. Remote control of insulin secretion by fat cells in Drosophila. Cell Metab. 2009; 10:199–207. [PubMed: 19723496]

10. Rajan A, Perrimon N. Drosophila cytokine unpaired 2 regulates physiological homeostasis by remotely controlling insulin secretion. Cell. 2012; 151:123–137. [PubMed: 23021220]
11. Thompson SN. Trehalose - The Insect Blood Sugar. Adv Insect Phys. 2003; 31:205–285.
12. Musselman LP, et al. A high-sugar diet produces obesity and insulin resistance in wild-type Drosophila. Disease models & mechanisms. 2011; 4:842–849. [PubMed: 21719444]
13. Braco JT, Gillespie EL, Alberto GE, Brenman JE, Johnson EC. Energy-dependent modulation of glucagon-like signaling in Drosophila via the AMP-activated protein kinase. Genetics. 2012; 192:457–466. [PubMed: 22798489]
14. Zhang H, et al. Deletion of Drosophila insulin-like peptides causes growth defects and metabolic abnormalities. Proc Natl Acad Sci U S A. 2009; 106:19617–19622. [PubMed: 19887630]
15. Gronke S, Clarke DF, Broughton S, Andrews TD, Partridge L. Molecular evolution and functional characterization of Drosophila insulin-like peptides. PLoS Genet. 2010; 6:e1000857. [PubMed: 20195512]
16. Crivat G, et al. Insulin stimulates translocation of human GLUT4 to the membrane in fat bodies of transgenic Drosophila melanogaster. PLoS One. 2013; 8:e77953. [PubMed: 24223128]
17. Becker A, Schloder P, Steele JE, Wegener G. The regulation of trehalose metabolism in insects. Experientia. 1996; 52:433–439. [PubMed: 8706810]
18. Chen Q, Haddad GG. Role of trehalose phosphate synthase and trehalose during hypoxia: from flies to mammals. The Journal of experimental biology. 2004; 207:3125–3129. [PubMed: 15299033]
19. Buch S, Melcher C, Bauer M, Katzenberger J, Pankratz MJ. Opposing effects of dietary protein and sugar regulate a transcriptional target of Drosophila insulin-like peptide signaling. Cell Metab. 2008; 7:321–332. [PubMed: 18396138]
20. Drucker DJ. The biology of incretin hormones. Cell Metab. 2006; 3:153–165. [PubMed: 16517403]
21. Sarkar S, Davies JE, Huang Z, Tunnacliffe A, Rubinsztein DC. Trehalose, a novel mTOR-independent autophagy enhancer, accelerates the clearance of mutant huntingtin and alpha-synuclein. J Biol Chem. 2007; 282:5641–5652. [PubMed: 17182613]
22. Higuchi T, Nishikawa J, Inoue H. Sucrose Induces Vesicle Accumulation and Autophagy. J Cell Biochem. 2014
23. Ikeya T, Galic M, Belawat P, Nairz K, Hafen E. Nutrient-dependent expression of insulin-like peptides from neuroendocrine cells in the CNS contributes to growth regulation in Drosophila. Curr Biol. 2002; 12:1293–1300. [PubMed: 12176357]
24. Arquier N, et al. Drosophila ALS regulates growth and metabolism through functional interaction with insulin-like peptides. Cell Metab. 2008; 7:333–338. [PubMed: 18396139]
25. Okamoto N, et al. A secreted decoy of InR antagonizes insulin/IGF signaling to restrict body growth in Drosophila. Genes Dev. 2013; 27:87–97. [PubMed: 23307869]
26. Kubota H, et al. Temporal coding of insulin action through multiplexing of the AKT pathway. Mol Cell. 2012; 46:820–832. [PubMed: 22633957]
27. Pasco MY, Leopold P. High sugar-induced insulin resistance in Drosophila relies on the lipocalin Neural Lazarillo. PLoS One. 2012; 7:e36583. [PubMed: 22567167]
28. Melo RC, Liu L, Xenakis JJ, Spencer LA. Eosinophil-derived cytokines in health and disease: unraveling novel mechanisms of selective secretion. Allergy. 2013; 68:274–284. [PubMed: 23347072]
29. Verhage M, et al. Differential release of amino acids, neuropeptides, and catecholamines from isolated nerve terminals. Neuron. 1991; 6:517–524. [PubMed: 2015091]
30. Xie L, Zhu D, Gaisano HY. Role of mammalian homologue of Caenorhabditis elegans unc-13-1 (Munc13-1) in the recruitment of newcomer insulin granules in both first and second phases of glucose-stimulated insulin secretion in mouse islets. Diabetologia. 2012; 55:2693–2702. [PubMed: 22814762]
31. Kwak SJ, et al. Drosophila adiponectin receptor in insulin producing cells regulates glucose and lipid metabolism by controlling insulin secretion. PLoS One. 2013; 8:e68641. [PubMed: 23874700]

32. Gronke S, et al. Dual lipolytic control of body fat storage and mobilization in Drosophila. PLoS Biol. 2007; 5:e137. [PubMed: 17488184]

33. Chang YY, Neufeld TP. An Atg1/Atg13 complex with multiple roles in TOR-mediated autophagy regulation. Mol Biol Cell. 2009; 20:2004–2014. [PubMed: 19225150]

34. Veenstra JA, Agricola HJ, Sellami A. Regulatory peptides in fruit fly midgut. Cell Tissue Res. 2008; 334:499–516. [PubMed: 18972134]

35. Tennessen JM, Barry WE, Cox J, Thummel CS. Methods for studying metabolism in Drosophila. Methods. 2014; 68:105–115. [PubMed: 24631891]

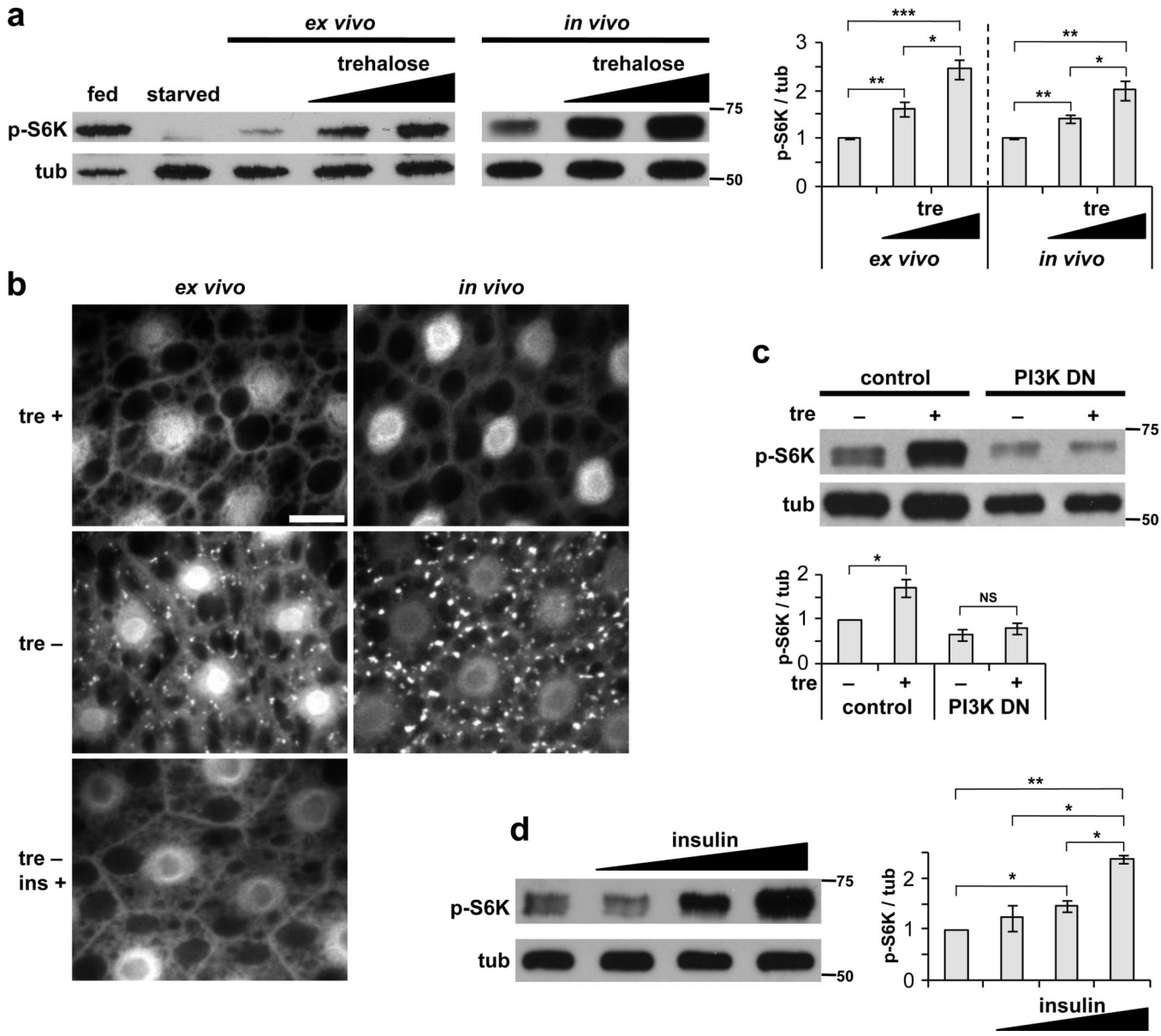

Figure 1. Trehalose promotes TOR signaling in the larval fat body

(a) TOR activity was measured by immunoblot of wild type fat body extracts with phospho-T398 S6K (p-S6K) antibody. Fed and starved controls (lanes 1 and 2) show the range of fb-TOR activity on standard fly food and following 2-hr starvation. In both *ex vivo* (larval carcasses incubated 2 hours in M3 medium with 0, 20 or 40 mg/ml trehalose) and *in vivo* (larvae cultured overnight in agar/tryptone food with 0, 13.3 or 26.6 mg/ml trehalose) cultures, addition of trehalose (tre) results in a dose-dependent increase in p-S6K. Data represent mean±s.e.m. of four independent experiments. **(b)** Trehalose inhibits formation of autophagic vesicles in larval fat body cells. *Cg-Gal4 / UAS-mCherry-Atg8a* carcasses or larvae were incubated under *ex vivo* (4 hr in M3 medium +/−20 mg/ml trehalose) or *in vivo* (overnight on agar/tryptone food +/−26.6 mg/ml trehalose) conditions. Human insulin (ins, 10 μg/ml) inhibits autophagosome formation in *ex vivo* cultures lacking trehalose. Scale bar

represents 20 μm. Images are representative of three experiments (seven larvae per condition). **(c)** PI 3-kinase activity is required for *ex vivo* activation of fb-TOR by trehalose. Expression of dominant negative p110 catalytic subunit in the fat body *(Cg-GAL4 / UAS-$p110^{D954A}$)* reduces fb-TOR activity and inhibits its response to trehalose. Data represent mean±s.e.m. of three independent experiments. **(d)** Addition of human insulin (0.01, 0.1, and 1 μg/ml) to *ex vivo* cultures lacking trehalose causes dose-dependent increases in fb-TOR activity. Data represent mean±s.e.m. of three independent experiments. Graphs display ratios of p-S6K/tubulin (tub) band intensities, normalized to control. *$p<0.05$, **$p<0.01$, ***$p<0.001$, NS $p>0.05$; Student's *t*-test. Full-size immunoblots are presented in Supplementary Figure 4.

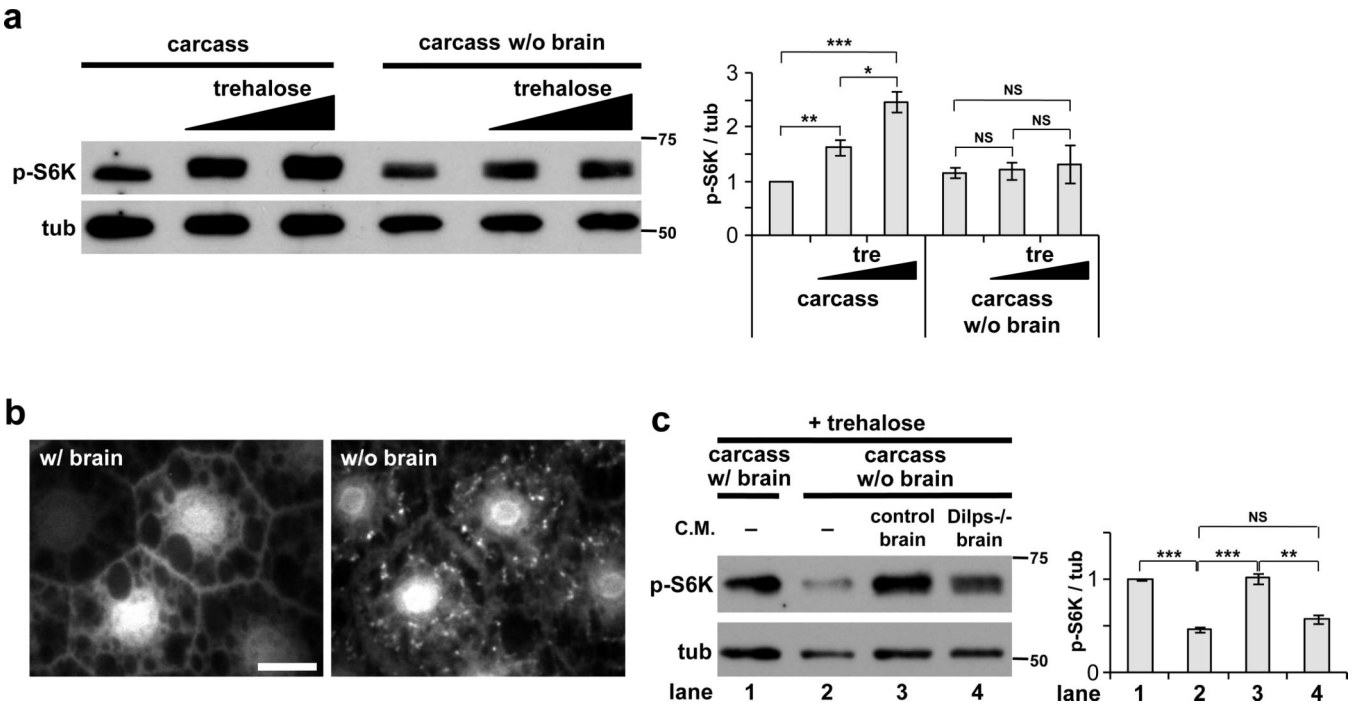

Figure 2. Trehalose-dependent activation of TOR in the larval fat body requires the brain and insulin signaling

(a) Supplementation of M3 medium with trehalose (0, 20, 40 mg/ml) leads to significant increases in fb-TOR activity from whole larval carcasses (left) but not in carcasses from which the brain was surgically removed (right). Data represent mean±s.e.m. of four independent experiments. **(b)** Trehalose (20 mg/ml in M3) suppresses formation of autophagic vesicles (mCherry-Atg8 punctae) in fat body cells of complete carcasses but not carcasses lacking the brain. Scale bar represents 20 μm. Representative images of three experiments (seven carcasses per condition). **(c)** Fb-TOR activity of carcasses lacking the brain, incubated in control M3+trehalose medium (−), or in M3+trehalose conditioned medium (C.M.) previously incubated 2h with CNS complexes from wild type larvae (control brain) or from mutant larvae lacking *Dilps1–5* and *Dilp7* (Dilps$^{-/-}$ brain). Data represent mean±s.e.m. of four independent experiments. *p<0.05, **p<0.01, ***p<0.001, NS p>0.05; Student's *t*-test. Full-size immunoblots are shown in Supplementary Figure 4.

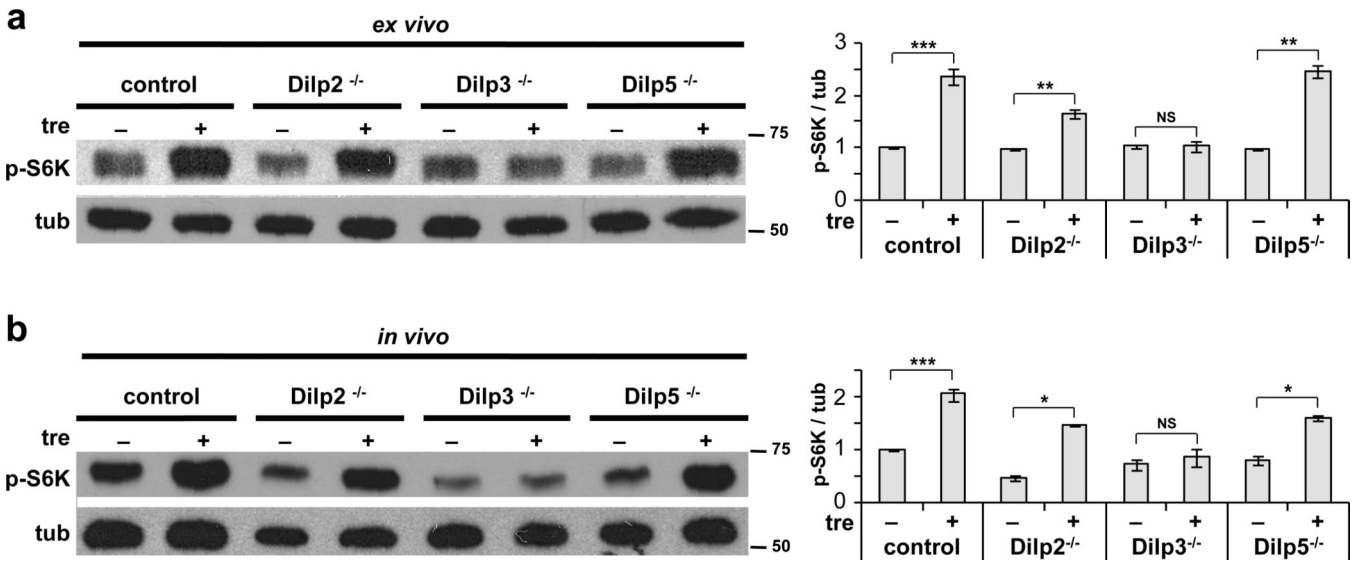

Figure 3. Dilp3 is required for TOR activation by trehalose

(a) *Ex vivo* incubation of larval carcasses in M3 medium supplemented with or without 40 mg/ml trehalose. Trehalose promotes fb-TOR activity in control, *Dilp2*$^{-/-}$ and *Dilp5*$^{-/-}$ larvae, but not in *Dilp3*$^{-/-}$ larvae. **(b)** *In vivo* incubation of larvae in agar/tryptone food containing 0 or 26.6 mg/ml trehalose. Fb-TOR activity is significantly increased by trehalose in control, *Dilp2*$^{-/-}$ and *Dilp5*$^{-/-}$ larvae, but not in *Dilp3*$^{-/-}$ larvae. Representative blots of three independent experiments are shown in each panel. Data were assessed by Student's *t*-test and are represented as mean±s.d. *p<0.05, **p<0.01, ***p<0.001, NS p>0.05. Full-size immunoblots are presented in Supplementary Figure 5.

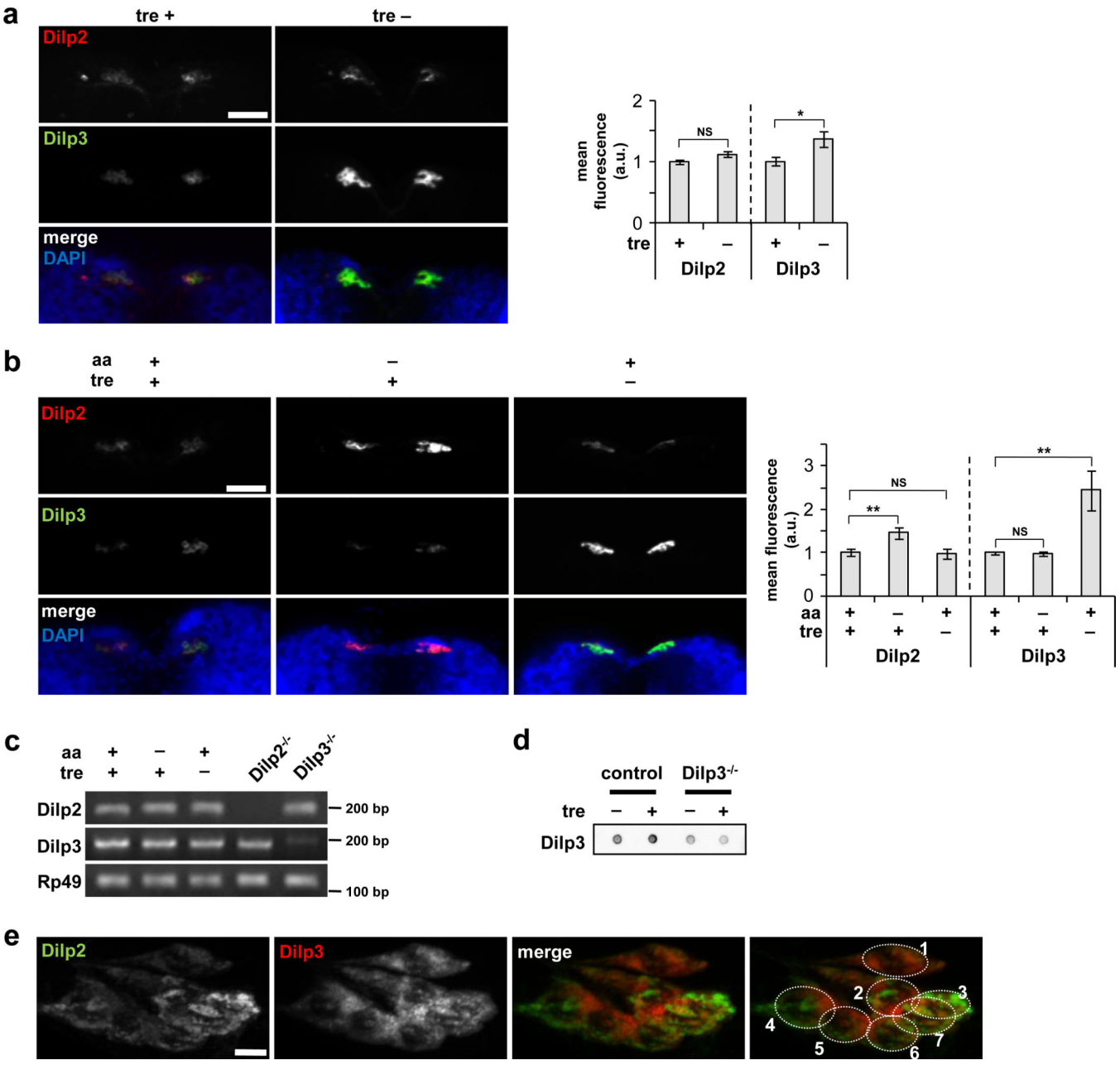

Figure 4. Trehalose promotes secretion of Dilp3

(a) Confocal images showing Dilp2 and Dilp3 protein following *ex vivo* incubation in the presence or absence of trehalose. Incubation in medium lacking trehalose leads to Dilp3 accumulation in the IPCs, whereas Dilp2 staining remains low under both conditions. **(b)** Accumulation of Dilp2 and Dilp3 in response to *in vivo* starvation for amino acids (aa) or trehalose. Levels of Dilp2 and Dilp3 are low in the IPCs of larvae raised on agar/tryptone/trehalose food. Dilp2 accumulates in response to lack of dietary amino acids (tryptone) but not trehalose, whereas Dilp3 accumulates in larvae raised on food lacking trehalose but not amino acids. Images in a and b are representative of eight larvae. Data were assessed by Student's *t*-test and are represented as mean±s.d. *p<0.05, **p<0.01, NS p>0.05. a.u.,

arbitrary units. **(c)** Levels of *Dilp2* and *Dilp3* mRNA in response to *in vivo* starvation for amino acids or trehalose, analyzed by semi-quantitative RT-PCR. *Rp49* serves as internal control. Representative results of three independent experiments are shown. **(d)** Dot blot analysis of circulating Dilp3 levels in larvae grown on food with or without trehalose *in vivo*. Blot is representative of three independent experiments. **(e)** High-magnification combined Z-series stack of confocal sections of IPCs from 24 hr starved larvae, demonstrating distinct intracellular localization and biased expression of Dilp2 and Dilp3. Image is representative of three experiments, n = 7 larvae. Scale bars represent 50 μm in (a) and (b), and 5 μm in (e). Full-size gel and dot blot scans are presented in Supplementary Figure 5.

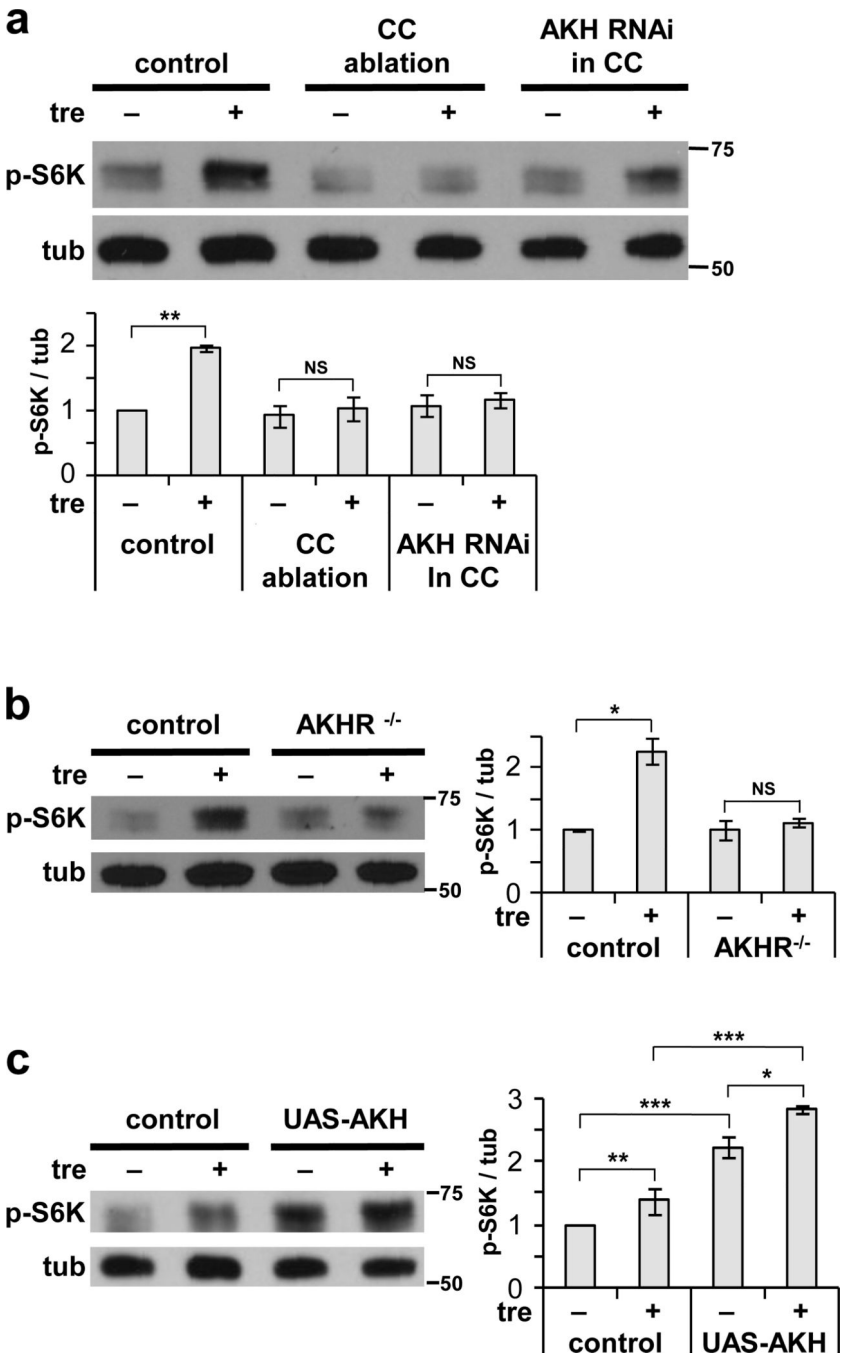

Figure 5. Activation of TOR by trehalose requires AKH signaling

(a, b) Trehalose-mediated *ex vivo* activation of fb-TOR is disrupted by ablation of the CC *(AKH-GAL4 / UAS-reaper)* or depletion of *AKH* from the CC *(AKH-GAL4 / UAS-AKH^{RNAi})* and by null mutation of the AKH receptor *(AKHR^{1}/AKHR^{1})*. **(c)** Overexpression of AKH *(Cg-GAL4 / UAS-Akh)* increases fb-TOR signaling in the presence and absence of trehalose *ex vivo*. Data represent mean±s.e.m. of three (a, b) or four (c) independent experiments. *p<0.05, **p<0.01, ***p<0.001, NS p>0.05; Student's *t*-test. Full-size immunoblots are presented in Supplementary Figure 5.

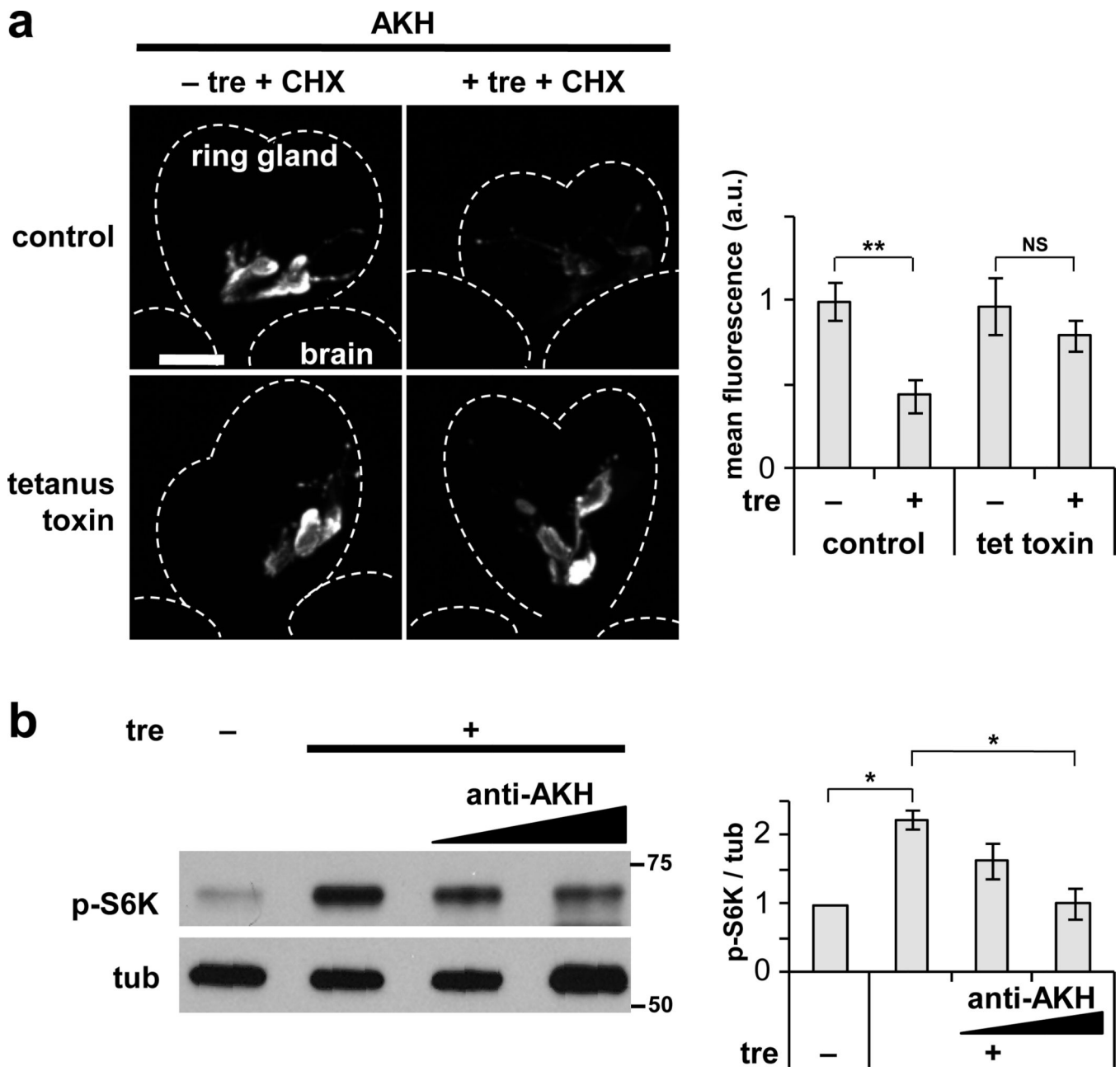

Figure 6. Trehalose promotes AKH secretion to stimulate fb-TOR signaling

(a) AKH antibody staining in the CC is reduced in response to trehalose during *ex vivo* incubation. CC-specific expression of tetanus toxin *(AKH-GAL4 / UAS-TeTxLC)* prevents the effect of trehalose. Cycloheximide (25 ug / ml) was included in all incubations to block AKH synthesis. Scale bar represents 50 μm. Representative images of seven ring glands per experimental condition are shown. **(b)** *Ex vivo* activation of fb-TOR signaling in response to trehalose is inhibited by blocking antibody against AKH (2×10^{-3} and 4×10^{-3} serum dilution in M3 media). Blot is representative of three independent experiments. Bar graphs in a and b represent mean±s.e.m. *p<0.05, **p<0.01, NS p>0.05; Student's *t*-test. Full-size immunoblots are shown in Supplementary Fig. 6.

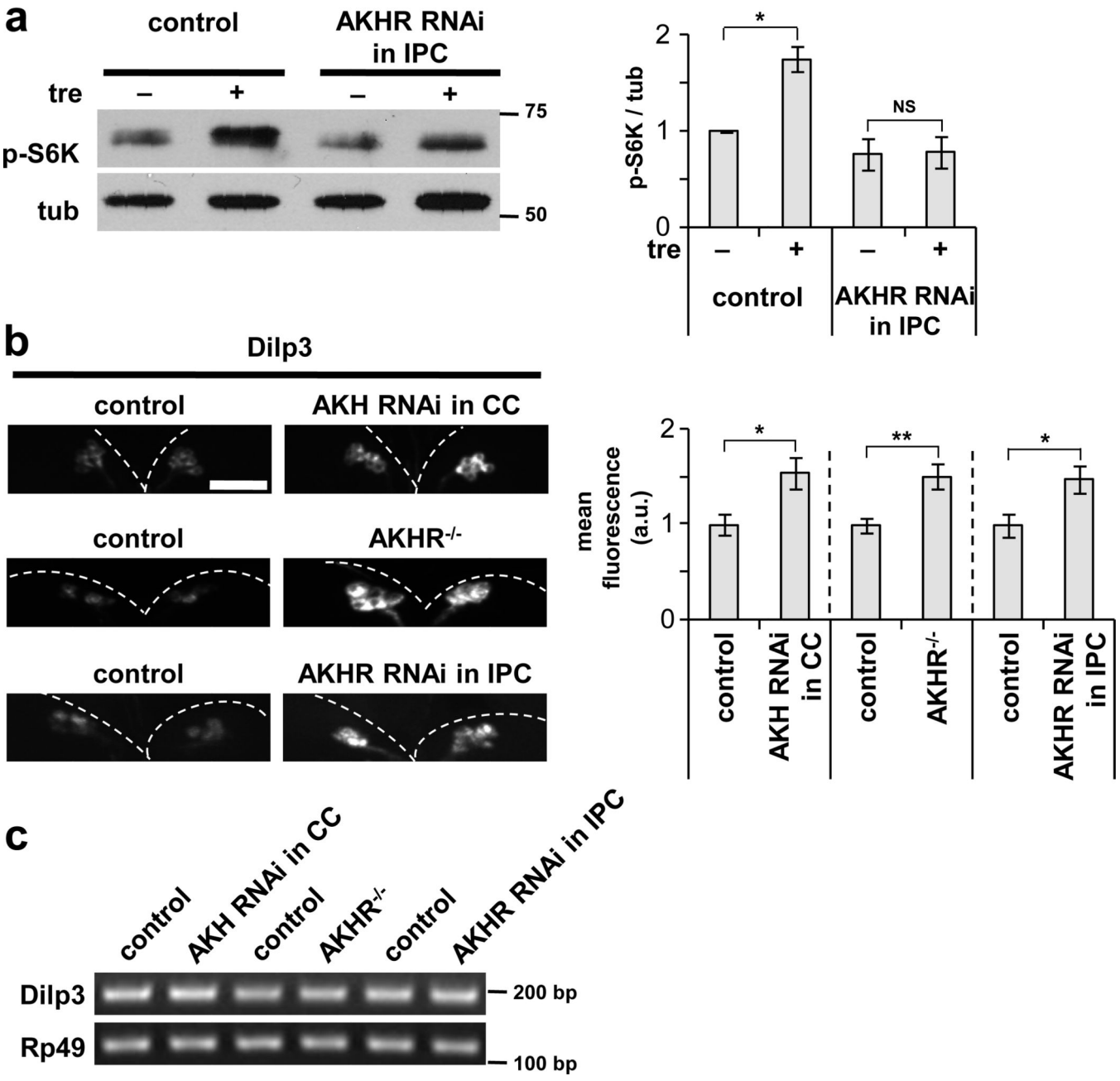

Figure 7. AKH signaling in the IPCs is required for Dilp3 release

(a) Depletion of *AKHR* by RNAi in the IPCs *(Dilp2-GAL4 / UAS-AKHR^{RNAi})* impairs TOR activation in the fat body in response to trehalose in the media. Blot is representative of three independent experiments. **(b)** Following *ex vivo* incubation in the presence of trehalose, Dilp3 protein accumulates in the IPCs in response to depletion of *AKH* in the CC *(AKH-GAL4 / UAS-AKH^{RNAi})*, null mutation of *AKHR (AKHR^{1}/Df (2L)Exel7027)*, and depletion of *AHKR* in the IPCs *(Dilp2-GAL4 / UAS-AKHR^{RNAi})*. Scale bar represents 50 μm. Representative images of eight animals per genotype are shown. Data in a and b were assessed by Student's *t*-test and are represented as mean±s.d. *p<0.05, **p<0.01, NS p>0.05. **(c)** Levels of *Dilp3* mRNA in the genotypes indicated in (b), analyzed by semi-

quantitative RT-PCR. *Rp49* serves as internal control. Blot is representative of three independent experiments. Full-size immunoblots and gels are presented in Supplementary Figure 6.

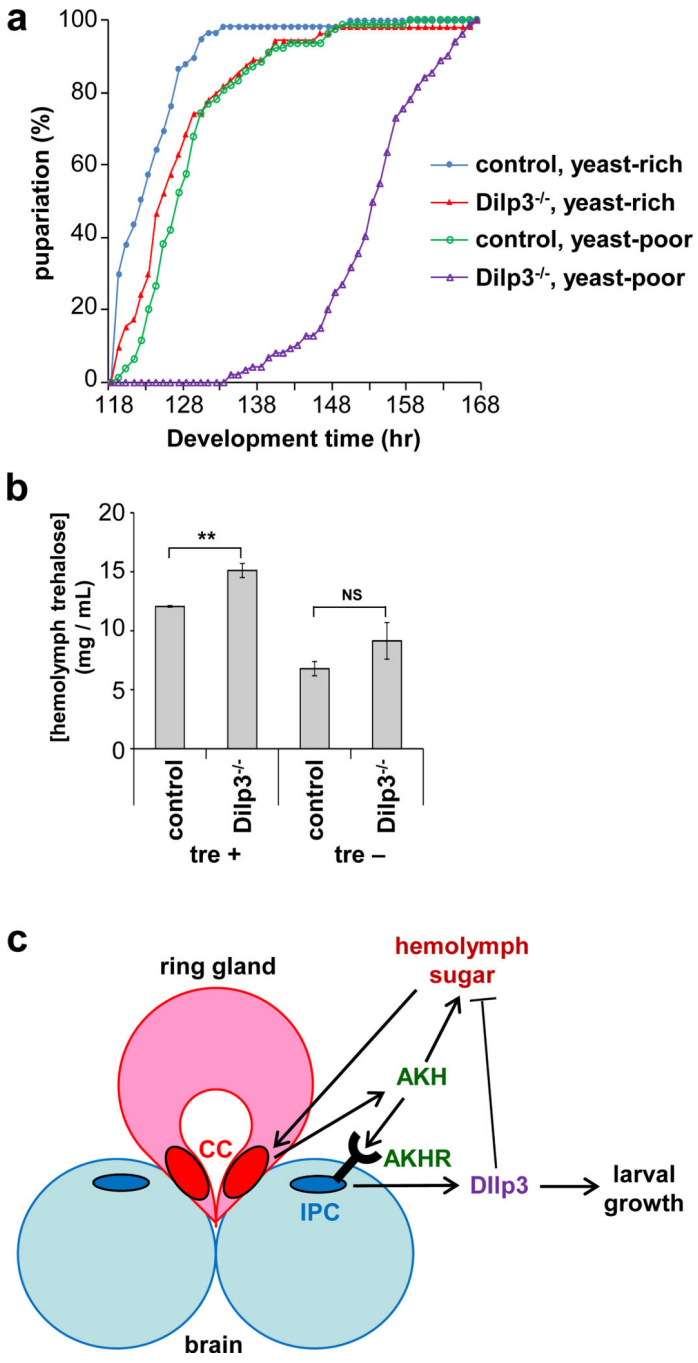

Figure 8. Dilp3 affects larval growth and sugar homeostasis

(a) Developmental timing from egg laying to pupariation of control and *Dilp3*$^{-/-}$ mutants raised on rich and poor medium (standard fly food with and without supplementary yeast, respectively). Data are from three vials of 30 larvae for each experimental condition. **(b)** Levels of circulating trehalose in control and *Dilp3*$^{-/-}$ larvae cultured in the presence or absence of trehalose *in vivo*. Data of three independent experiments were assessed by Student's *t*-test and are represented as mean±s.d. **p<0.01, NS p>0.05. **(c)** The results are consistent with a model whereby sugar stimulates release of AKH from the CC, which then

triggers secretion of Dilp3 from the IPCs. Increased insulin signaling in peripheral tissues promotes larval growth, sugar uptake, and activation of TOR in the fat body, the latter of which may lead to further signal amplification through subsequent stimulation of Dilp2 release from the IPCs. The sugar-dependent secretion of AKH represents another potential positive feedback loop, which may be restricted by the counterbalancing effect of Dilp3. This model implies that in rapidly growing Drosophila larvae, co-regulation of AKH and insulin signaling may support high rates of insulin-dependent anabolic growth while preventing excessive storage of trehalose in the fat body, allowing other cells to use sugar to fuel cell growth.